Journal on Materials and its Characterization

Vol: 4(2), June 2025

REST Publisher; ISBN: 2583-6412

Website: http://restpublisher.com/journals/jmc/

DOI: https://doi.org/10.46632/jmc/4/2/4

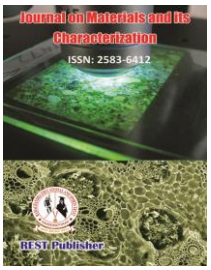

Brain Multiple Sclerosis Detection: A Deep Learning Approach with VGG16 and Data Augmentation

*** S. M. Zakariya, Mohammad Sarosh Umar**

Aligarh Mulsim University, Aligarh, India.

** Corresponding author Email: rupali.asc@quantumeducation.in*

Abstract: *Multiple Sclerosis (MS) is a chronic autoimmune disease affecting the central nervous system, characterized by demyelination and resulting in a range of neurological impairments. While MRI is the primary imaging modality for diagnosis, manual interpretation is time-consuming and subjective. This study presents an automated deep learning approach to classify brain MRI scans for MS detection, leveraging a VGG16-based Convolutional Neural Network (CNN) enhanced via transfer learning. The model classifies images into four categories: Control-Axial, Control-Sagittal, MS-Axial, and MS-Sagittal. We evaluated the model under two scenarios: using an original dataset of 3,427 MRI images and an augmented dataset of 6,000 images. The model trained on the augmented dataset achieved superior performance with 98.09% test accuracy and 99.87% AUC, compared to 94.44% and 99.13% respectively without augmentation. Precision and recall across all classes exceeded 0.93, and ROC curves showed near-perfect separability, particularly improving distinction between MS and control in axial views. These findings suggest that deep learning, especially when paired with data augmentation, offers a reliable and efficient tool for MS detection. Future work will explore multimodal data integration and robust validation across diverse patient cohorts to support clinical deployment.*

Keywords: *multiple sclerosis, deep learning, convolutional neural networks, VGG16, MRI brain scans, automated detection, medical image classification, data augmentation.*

1. INTRODUCTION

Multiple Sclerosis (MS) is a long-term autoimmune disorder that impacts the central nervous system (CNS), marked by inflammation and damage to the myelin sheath that surrounds nerve fibers. This loss of myelin results in a wide range of neurological symptoms such as motor difficulties, sensory impairments, and cognitive issues. Early and precise diagnosis is essential for optimal disease management. Magnetic Resonance Imaging (MRI) remains the primary method for detecting MS-related lesions, thanks to its ability to highlight hyperintense areas of demyelination. However, Conventional MRI analysis relies on expert evaluation, which may cause inconsistencies and delays in diagnosis [1].

Deep learning, particularly Convolutional Neural Networks (CNNs), has revolutionized medical imaging, especially in MRI analysis. CNNs excel at identifying complex patterns and detecting MS lesions faster and more consistently than radiologists, even spotting subtle features that might be overlooked, leading to more objective clinical assessments [2]. Developing effective CNN models for MS detection is challenging due to the high variability in MRI datasets, caused by differences in imaging protocols, scanner hardware, and patient anatomy. This variability limits model generalizability across settings. Standard preprocessing steps, like image normalization and resizing, are crucial, while data augmentation improves robustness by adding synthetic diversity. Transfer learning helps overcome the limited availability of annotated MS data by fine-tuning pre-trained models on smaller labeled datasets [3], [4].

Model interpretability is crucial in clinical AI, especially in fields like neurology, where clinicians need to understand automated decision-making. Visual explanation tools like saliency maps and Grad-CAM highlight key MRI regions influencing model outputs. These tools build clinician trust and allow for verification with radiological findings, aiding AI adoption [5], [6]. MS has various forms, such as relapsing-remitting and primary progressive MS, each with distinct progression patterns and treatment needs [7]. Ongoing research aims to identify biomarkers for improved subtype classification and personalized treatments [8]. Given the volume and complexity of modern imaging data, there is a growing need for automated tools to assist radiologists. Manual lesion detection is time-intensive and susceptible to observer bias, particularly in regions with limited specialist availability. Integrating AI into diagnostic workflows can streamline image review, highlight candidate lesion regions, quantify lesion volumes, and facilitate longitudinal monitoring. These capabilities may ultimately reduce diagnostic delays and improve consistency across practitioners [9], [10].

This study explores using a VGG16-based CNN for automated MS detection in brain MRI scans through transfer learning. The model performs binary classification to distinguish MS from non-MS cases and is evaluated with both original and augmented datasets. Standard preprocessing steps, such as normalization and resizing, are applied. The goal is to assess the feasibility of deep learning for scalable, reliable MS diagnosis.
Methodology

This research utilizes a VGG16-based Convolutional Neural Network (CNN) to autonomously identify Multiple Sclerosis (MS) in MRI brain images. By applying transfer learning, the pre-trained VGG16 architecture is adapted and refined for binary classification distinguishing MS cases from non-MS ones. The experimental framework comprises two distinct configurations: the first employs the raw dataset, while the second integrates data augmentation strategies to bolster the model's capacity for generalization.

Convolutional Neural Network (CNN)
A Convolutional Neural Network (CNN) is a neural network designed for processing grid-like data, especially images. It excels in image classification, object detection, and segmentation by recognizing spatial hierarchies in data [11]. CNNs consist of convolutional, pooling, and fully connected layers. Convolutional layers use filters to extract features like edges and textures, creating feature maps [12]. Pooling layers reduce dimensions to lower computational load and prevent overfitting, with max pooling commonly used [13]. After several convolution and pooling stages, the flattened features are passed to fully connected layers for predictions [14]. Techniques like dropout and batch normalization further improve performance. CNNs are particularly effective in visual recognition, advancing fields like deep learning and computer vision [15].

VGG16-CNN
VGG16, developed by the University of Oxford's Visual Geometry Group, gained fame by excelling in the 2014 ImageNet Challenge. It has 16 layers, including 13 convolutional and 3 fully connected layers [16]. Small 3x3 filters in the convolutional layers efficiently capture detailed features, while max pooling reduces spatial resolution to highlight key image aspects [17], [18]. ReLU activations enable non-linear learning, and the fully connected layers classify the features [19], [20]. Though computationally intensive, VGG16 is widely used in transfer learning to boost performance on smaller datasets [21]. Its design influences many modern CNN architectures and remains relevant in tasks like object detection and feature extraction [22].

2. RESULTS AND DISCUSSION

The results of the study are evaluated based on the following metrics: Accuracy, Precision, Recall, F1-Score, Loss, and ROC value. These metrics are defined as follows [23], [24]:
Accuracy is the proportion of correctly classified instances from the total dataset.

$$Accuracy = \frac{TruePositive+TrueNegative}{TruePositive+TrueNegative+FalsePositive+FalseNegative} \quad (1)$$

Precision is the ratio of true positives vs. a total number of positive predictions. It measures how well the model avoids false positives.

$$Precision = \frac{TruePositive}{TruePositive+FalsePositive} \quad (2)$$

Recall is the ratio of true positive vs. total number of actual positive instances. It measures the model's ability to identify all relevant cases correctly.

$$Recall = \frac{TruePositive}{TruePositive+FalseNegative} \quad (3)$$

F1-score is the harmonic mean of precision and recall. It provides a single score that considers both false positives and false negatives. It is calculated as follows:

$$F1-Score = 2\,x\,\frac{Precision\ x\ Recall}{Precision+Recall} \quad (4)$$

Loss is the measure of inconsistency between predicted and actual class labels, computed by means of appropriate loss functions such as categorical cross-entropy loss. In a CNN, the loss function measures how closely the model's predictions align with the actual labels in the training data. Loss is calculated as follows:

$$Loss = -\sum_{i=1}^{C} y_i * \log[\hat{y}_i] \quad (5)$$

Where: c is the number of classes, y_i is the actual probability that it fits to class i and $\hat{y}_i$ is the predicted probability that fits into class i

True Positive Rate (TPR) or Sensitivity: Plotted on the y-axis, this is the proportion of actual positives that are correctly identified (i.e., how many tumors are correctly identified by the model).

$$TPR = \frac{TruePositive}{(TruePositive + FalseNegative)} \quad (6)$$

False Positive Rate (FPR): Plotted on the x-axis, this is the proportion of actual negatives that are incorrectly identified as positive (i.e., how many non-tumor cases are falsely classified as tumors).

$$FPR = \frac{FalsePositive}{(FalsePositive+TrueNegative)} \quad (7)$$

The ROC curve shows the trade-off between the True and False Positive rates.

VGG16-CNN model without Augmentation

The dataset is split into training (80%), validation (10%), and test (10%) sets to ensure effective model evaluation. The image distribution across various brain multiple sclerosis classes in each subset and the comprehensive full dataset is shown in Table I for better understanding.

Table II summarizes the VGG16 model's performance without data augmentation during key training phases. At Epoch 1, the model had limited capability (accuracy: 55.19%, AUC: 0.7944), marking the start of its learning curve. By Epoch 8—its optimal validation stage—it achieved 95.07% accuracy and a low loss of 0.1443, indicating effective feature extraction. Final training outcomes neared ideal values, signaling a well-fitted model. Test metrics remained high (accuracy: 94.44%, AUC: 0.9913), demonstrating strong generalization.

Fig. 1 illustrates the performance of the VGG16-CNN model trained without data augmentation over 11 epochs. Training accuracy rose rapidly from 55.19% in the first epoch to over 93% by the fifth, with AUC scores reaching 99.45% and training loss consistently decreasing. By epoch 8, validation metrics achieved 95.07% accuracy and 99.27% AUC, indicating strong generalization.

TABLE 1. Distribution of images across each class in the Complete, Training, Validation, and Test Dataset

Class	**Train Data**	**Validation Data**	**Test Data**	**Complete Data**
Control-Axial	801	101	100	1002
Control-Sagittal	811	102	101	1014
MS-Sagittal	608	77	76	761
MS-Axial	520	65	65	650
Total	**2740**	**345**	**342**	**3427**

TABLE 2. VGG16 Model Performance without Data Augmentation.

Phase	Accuracy (%)	AUC	Loss	Precision (%)	Recall (%)
Epoch 1	55.19	0.7944	1.2726	55.14	38.64
Best Val	95.07	0.9927	0.1443	95.07	95.07
Final Train	99.23	0.9998	0.044	99.15	99.15
Final Test	94.44	0.9913	0.198	94.44	94.44

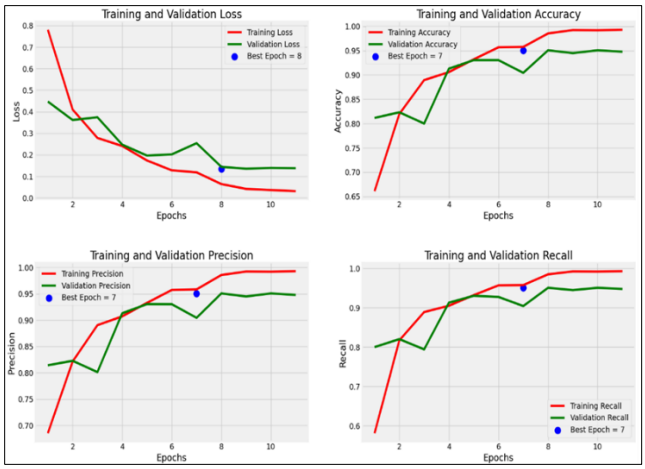

FIGURE 1. Epoch-wise Comparison of Loss, Accuracy, Precision, and Recall for Training and Validation Sets in VGG16 Model without Data Augmentation.

Throughout the epochs, training and validation accuracy, precision, and recall steadily improved. However, after the eighth epoch, a gap emerged between training and validation trajectories, subtly indicating the onset of overfitting.

Table III shows the final evaluation of the VGG16-CNN model without augmentation, demonstrating strong performance. It achieved 99.23% training accuracy with a low loss of 0.0440 and an AUC of 99.98%. On the test set, the model maintained high accuracy at 94.44%, with a loss of 0.1980 and an AUC of 99.13%, indicating excellent discrimination between MS and non-MS. The slight drop in performance from training to testing suggests minor overfitting, which could be mitigated using data augmentation or regularization techniques.
Table IV summarizes classification performance across four categories. The model achieves high precision for MS-Axial and Control-Sagittal (both 0.97) and the highest recall for Control-Axial (0.99), while MS-Axial has lower recall (0.86). All classes maintain strong F1-scores (≥0.91), indicating robust performance, though MS-Axial may need further data or tuning to boost recall.

TABLE 3. Performance Summary – VGG16 Model Without Augmentation.

Metric	Training Set	Test Set
Loss	0.044	0.198
Accuracy	99.23%	94.44%
AUC	99.98%	99.13%

TABLE 4. Per-Class Classification Report - VGG16 Model: Precision, Recall, and F1-Score Analysis.

Class	Precision	Recall	F1-Score	Support
Control-Axial	0.92	0.99	0.95	100
Control-Sagittal	0.97	0.95	0.96	101
MS-Axial	0.97	0.86	0.91	65
MS-Sagittal	0.94	0.95	0.94	76

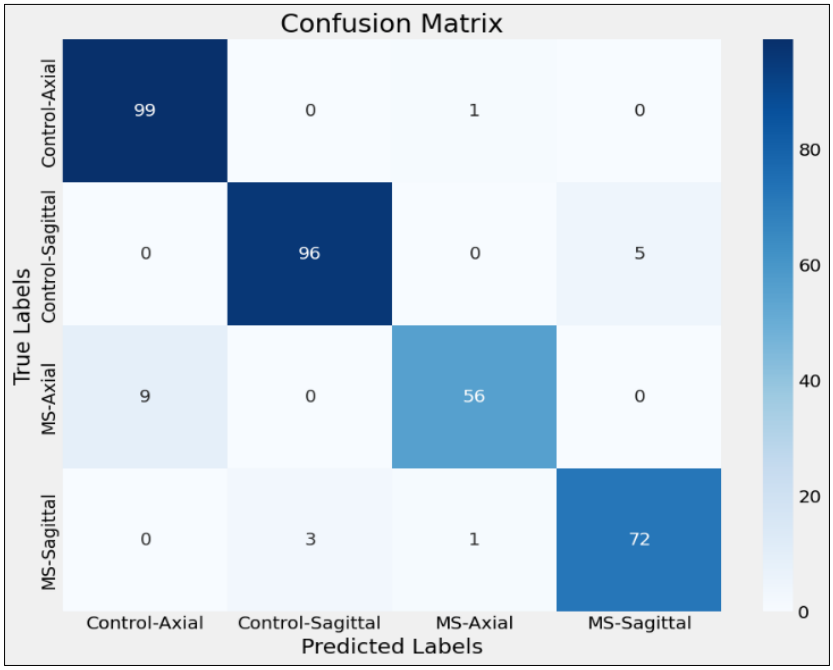

FIGURE 2. Confusion Matrix for Multi-Class Classification of Control and MS Images.

The confusion matrix shown in Fig. 2 conveys the classifier's effectiveness across four categories: Control-Axial, Control-Sagittal, MS-Axial, and MS-Sagittal. Strong diagonal values indicate high accuracy—Control-Axial at 99/100 and Control-Sagittal at 96/101. MS-Sagittal also performs well (72/76), but MS-Axial shows notable ambiguity, often misclassified as Control-Axial (9 times), leading to the lowest recall. Off-diagonal entries highlight these misclassifications, especially between MS-Axial and Control-Axial. This pattern suggests the potential benefit of refining or augmenting data to improve MS-Axial classification.

The ROC curves shown in Fig. 3 highlight the VGG16 model's strong performance across four MRI types: Control-Axial, Control-Sagittal, MS-Axial, and MS-Sagittal. Each curve significantly deviates from the diagonal, indicating performance well above random guessing. AUC scores confirm this: Control-Sagittal scores 1.00, Control-Axial and MS-Axial score 0.99, and MS-Sagittal scores 0.98. The model effectively distinguishes control from MS across both axial and sagittal views with minimal false positives. The slightly lower AUC for MS-Sagittal suggests potential for improved sensitivity to MS-related features in sagittal.

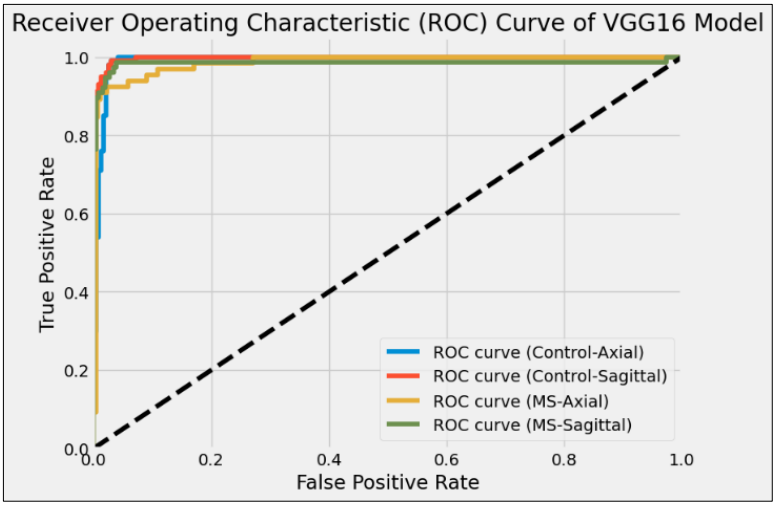

FIGURE 3. ROC Curve of VGG16 Model for Classifying Control and MS MRI Scans.

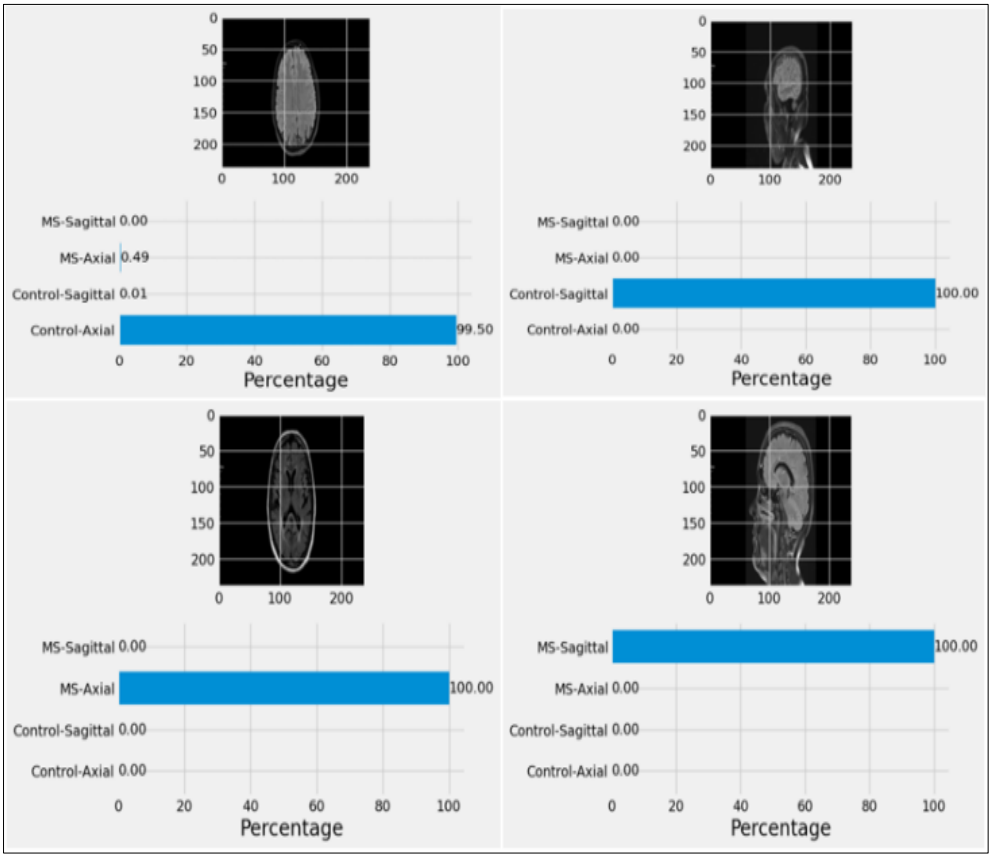

FIGURE 4. ROC Curve of VGG16 Model for Classifying Control and MS MRI Scans.

Figure 4 presents the VGG16 model's classification results for MRI scans across four categories: Control-Axial, Control-Sagittal, MS-Axial, and MS-Sagittal. Each panel pairs an MRI slice with a confidence bar graph, showing classification accuracies over 99%, such as 99.5% for Control-Axial and 100% for Control-Sagittal. The model achieved AUCs of 1.00 (Control-Sagittal), 0.99 (Control-Axial, MS-Axial), and 0.98 (MS-Sagittal), demonstrating strong performance without data augmentation. However, the lack of augmentation may affect generalizability, indicating a need for future improvements.

VGG16-CNN model with Augmentation

To improve model robustness and generalization, data augmentation techniques were applied, including flips, shear and zoom (0.2 range), shifts (0.1 range), and rotations up to 90°. Starting with 3,427 MRI images, augmentation expanded the dataset to 6,000 images by applying these transformations to a base of 1,500. This increased diversity and volume supported more effective training. Table V shows the distribution of augmented images across MS classes in the training, validation, test, and full datasets. Based on Table VI, the VGG16 model exhibited a marked enhancement in performance for MRI brain scan classification when data augmentation was applied. Initially, it recorded a modest training accuracy of 62.9% and an AUC of 0.84 at epoch 1. However, it swiftly escalated to near-optimal results, reaching a remarkable 99.9% training accuracy and a perfect AUC of 1.00 by the final epoch. Validation metrics mirrored this upward trend, culminating in a peak accuracy of 96.17% and an AUC of 0.9980. This progression reflects a pronounced improvement in generalization capabilities, largely attributed to the diversity introduced through augmentation.

TABLE 5. Distribution of images across each class in the Complete, Training, Validation, and Test Dataset

Class	**Train Data**	**Validation Data**	**Test Data**	**Complete Data**
Control-Axial	1200	150	150	1500
Control-Sagittal	1200	150	150	1500
MS-Sagittal	1200	150	150	1500
MS-Axial	1200	150	150	1500
Total	**4800**	**600**	**600**	**6000**

TABLE 6. VGG16 Model Performance with Data Augmentation.

Phase	Accuracy (%)	AUC	Loss	Precision (%)	Recall (%)
Epoch 1	62.91	0.8433	1.1174	63.45	60.23
Best Val	96.17	0.998	0.1077	96.17	96.17
Final Train	99.91	1	0.0115	99.91	99.91
Final Test	98.09	0.9987	0.075	98.09	98.09

Ultimately, the model's robustness was affirmed on the test dataset, where it attained 98.09% accuracy and an AUC of 0.9987, emphasizing how vital augmentation is in refining deep learning approaches for medical image analysis.

Fig. 5 displays the VGG16-CNN model's performance over 11 training epochs without data augmentation. The model learned quickly, with training accuracy rising from 55.19% to over 93% by epoch 5. AUC scores climbed steadily, reaching 99.45%, while training loss consistently declined. Validation performance peaked around epoch 8, with accuracy hitting 95.07% and AUC reaching 99.27%, reflecting strong generalization. Throughout training, accuracy, precision, and recall for both training and validation improved steadily. However, after epoch 8, a widening gap between training and validation trends suggested early signs of overfitting. Table VII shows the final evaluation of the VGG16 model with augmented data, highlighting excellent learning and generalization. The model achieved a low training loss (0.0119), near-perfect accuracy (99.81%), and a perfect AUC of 100%, indicating strong convergence. On the test set, it maintained 97.67% accuracy, 99.74% AUC, and a slight increase in loss (0.1009), demonstrating improved generalizability through data augmentation. These results confirm that augmentation enhanced both learning speed and model robustness for MRI classification.

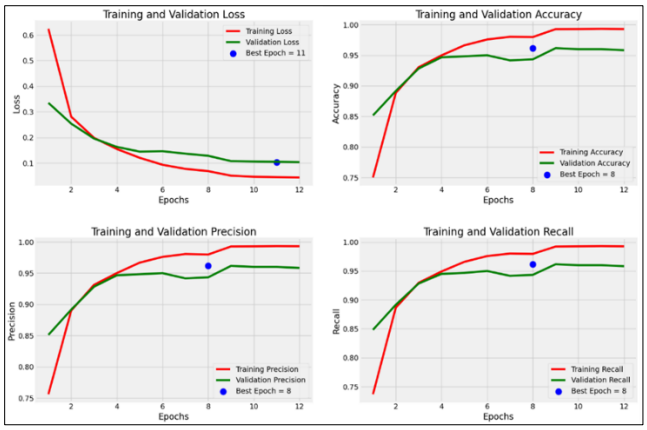

FIGURE 5. Epoch-wise Comparison of Loss, Accuracy, Precision, and Recall for Training and Validation Sets in VGG16 Model with Data Augmentation.

TABLE 7. Performance Summary – VGG16 Model With Data Augmentation.

Metric	Training Set	Test Set
Loss	0.0119	0.1009
Accuracy	99.81%	97.67%
AUC	100.00%	99.74%

Table VIII highlights the VGG16 model's excellent performance with augmented datasets across all categories. Control-Axial achieved perfect precision and high recall, while Control-Sagittal reached flawless recall, minimizing false negatives. MS-Axial demonstrated near-perfect precision and recall (~0.99), consistently identifying MS features. Although MS-Sagittal had a slightly lower recall (0.93), its precision remained perfect, avoiding mislabeling. The high F1-scores (≥0.97) across all categories confirm the model's strong, balanced performance, making it well-suited for clinical MRI-based MS diagnostics.

The confusion matrix shown in Fig. 6 illustrates the VGG16 model's strong performance across four MRI categories: Control-Axial, Control-Sagittal, MS-Axial, and MS-Sagittal. A clear diagonal trend highlights high accuracy. The model correctly classified 147 of 150 Control-Axial images, with minor confusion with MS-Axial.

Control-Sagittal was classified perfectly (150/150), and MS-Axial saw only one mislabeling. MS-Sagittal showed slightly more errors—9 mislabeled as Control-Sagittal and 1 as MS-Axial—suggesting feature similarities between sagittal views of MS and control cases.

Figure 7 shows the ROC curves of the VGG16 model, trained with data augmentation, for classifying MRI scans into Control and MS across axial and sagittal views. All curves trend sharply toward the top-left, indicating strong and consistent performance with high true positive rates and low false positives. This highlights the model's robust generalization and effectiveness in distinguishing MS from control cases.

TABLE 8. Per-Class Precision, Recall, and F1-Score for VGG16 Model With Data Augmentation.

Class	Precision	Recall	F1-Score	Support
Control-Axial	1	0.98	0.99	150
Control-Sagittal	0.94	1	0.97	150
MS-Axial	0.97	0.99	0.98	150
MS-Sagittal	1	0.93	0.97	150

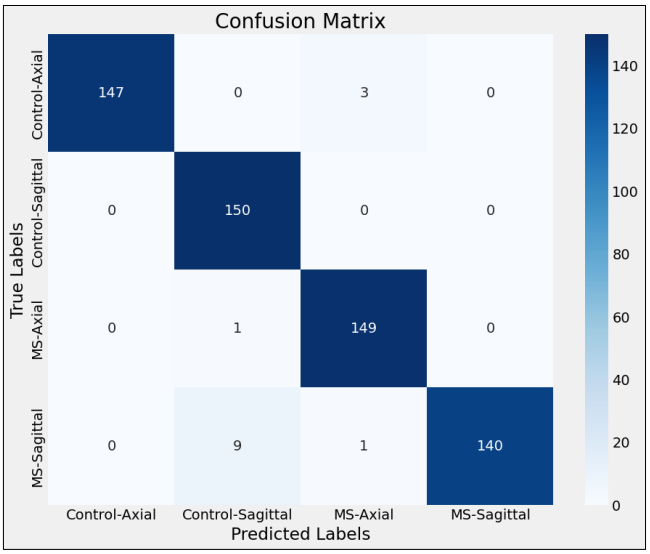

FIGURE 6. Confusion Matrix of VGG16 Model Performance on MRI Classification (With Augmentation).

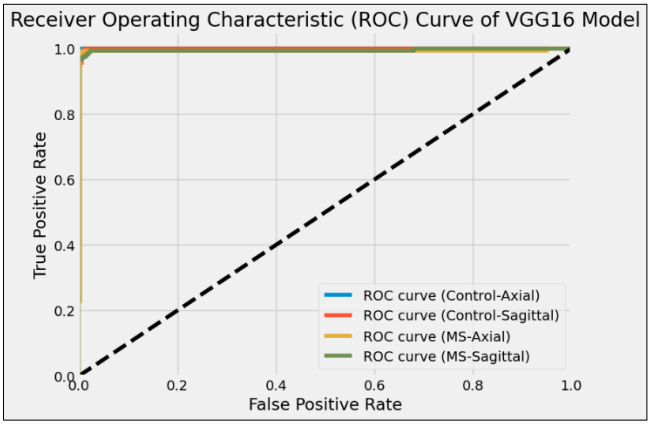

FIGURE 7. ROC Curve of VGG16 Model with Data Augmentation for Classifying Control and MS MRI Scans.

Fig. 8 shows VGG16 classification results on MRI slices—Control-Axial, Control-Sagittal, MS-Axial, and MS-Sagittal—after applying data augmentation. Each subplot displays the input image alongside predicted class probabilities. The model confidently classifies three of four slices with 100% certainty, with only one minor error: a Control-Axial image was slightly misclassified as MS-Axial (0.49%). Augmentation significantly improved performance by increasing data diversity and correcting class imbalance, expanding the dataset to 1,500 samples

per class. Without augmentation, VGG16 still achieved 94.44% accuracy and a 99.13% AUC, though overfitting emerged around epoch 8 due to limited data variability. With augmentation, performance rose to 98.09% accuracy and 99.87% AUC (Figure 9), and ROC curves clustered in the top-left corner—highlighting strong class discrimination across both MS diagnosis and scan orientation. Notably, prior confusion between MS and control axial scans was nearly eliminated.

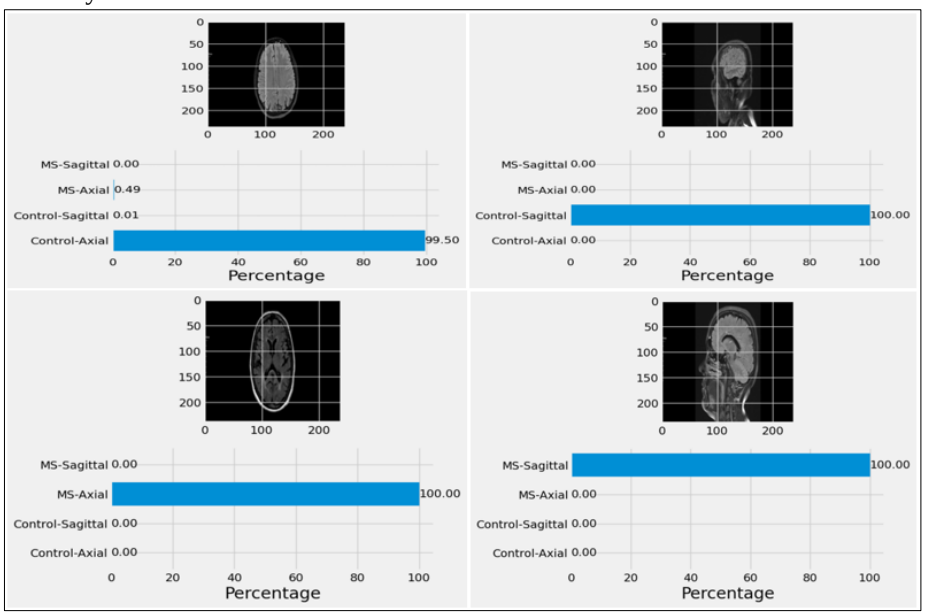

FIGURE 8. VGG16 Model (with Data Augmentation) Predictions for MRI Classification Across Control and MS Subtypes.

3. CONCLUSION

Multiple Sclerosis (MS) is a chronic autoimmune disorder affecting the central nervous system, leading to myelin degradation and neurological issues. Early and accurate diagnosis is essential, with MRI as the primary tool. However, traditional diagnostic methods face challenges like subjectivity, inefficiency, and growing imaging volumes. This study explores the use of deep learning—specifically VGG16-based Convolutional Neural Networks (CNNs)—to automatically detect MS from brain MRIs.

Experiments comparing models with and without data augmentation revealed key insights. Without augmentation, the model achieved 94.44% test accuracy and a 99.13% AUC but showed signs of overfitting after the eighth epoch. Adding data augmentation significantly improved results, boosting test accuracy to 98.09% and AUC to 99.87%, while reducing misclassification—especially between MS-Axial and Control-Axial images. Techniques like rotation, flipping, and zooming enhanced the model's ability to recognize MS features across varied views. Despite these promising outcomes, clinical adoption faces hurdles, including inconsistent MRI protocols, the need for interpretable AI, and broader validation. Still, this work demonstrates the strong potential of deep learning to aid radiologists by pre-screening images, highlighting abnormalities, and supporting faster diagnoses.

REFERENCES

[1]. A. Shoeibi et al., "Applications of deep learning techniques for automated multiple sclerosis detection using magnetic resonance imaging: A review," Comput Biol Med, vol. 136, p. 104697, 2021, doi: https://doi.org/10.1016/j.compbiomed.2021.104697.

[2]. A. Alijamaat, A. NikravanShalmani, and P. Bayat, "Multiple sclerosis identification in brain MRI images using wavelet convolutional neural networks," Int J Imaging Syst Technol, vol. 31, no. 2, pp. 778–785, Jun. 2021, doi: https://doi.org/10.1002/ima.22492.

[3]. P. Schwab and W. Karlen, "A Deep Learning Approach to Diagnosing Multiple Sclerosis from Smartphone Data," IEEE J Biomed Health Inform, vol. 25, no. 4, pp. 1284–1291, 2021, doi: https://10.1109/JBHI.2020.3021143.

[4]. E. Mohseni and S. M. Moghaddasi, "A Hybrid Approach for MS Diagnosis Through Nonlinear EEG Descriptors and Metaheuristic Optimized Classification Learning," Comput Intell Neurosci, vol. 2022, no. 1, p. 5430528, Jan. 2022, doi: https://doi.org/10.1155/2022/5430528.

[5]. M. P. McGinley, C. H. Goldschmidt, and A. D. Rae-Grant, "Diagnosis and Treatment of Multiple Sclerosis: A Review," JAMA, vol. 325, no. 8, pp. 765–779, Feb. 2021, doi: https://10.1001/jama.2020.26858.
[6]. W. Huang, W. Chen, and X. Zhang, "Multiple sclerosis: Pathology, diagnosis and treatments (Review)," Exp Ther Med, vol. 13, no. 6, pp. 3163–3166, 2017, doi: https://10.3892/etm.2017.4410.
[7]. B. Zakrzewska-Pniewska et al., "Update on diagnosis and treatment of neuromyelitis optica spectrum disorders (NMOSD) — recommendations of Section of Multiple Sclerosis and Neuroimmunology of Polish Neurological Society," Neurol Neurochir Pol, vol. 59, no. 1, pp. 6–19, 2025, doi: https://10.5603/pjnns.100945.
[8]. H. M. Rehan Afzal, S. Li, Y. Feng, M. K. Afzal, and P. Yang, "Enhancing multiple sclerosis diagnosis and prognosis through a dual Patch-Wise CNN architecture," Biomed Signal Process Control, vol. 107, p. 107835, 2025, doi: https://doi.org/10.1016/j.bspc.2025.107835.
[9]. G. Placidi et al., "A Context-Dependent CNN-Based Framework for Multiple Sclerosis Segmentation in MRI," Int J Neural Syst, vol. 35, no. 03, p. 2550006, Dec. 2024, doi: https://10.1142/S0129065725500066.
[10]. S. J. Basha, D. Veeraiah, P. C. Kumar, and P. C. K. Reddy, "Advancing Multiple Sclerosis Diagnosis: A CNN Approach for Personalized Therapy," in 2024 5th International Conference on Electronics and Sustainable Communication Systems (ICESC), 2024, pp. 1926–1931. doi: https://10.1109/ICESC60852.2024.10689766.
[11]. W. Brahmi, I. Jdey, and F. Drira, "Exploring the role of Convolutional Neural Networks (CNN) in dental radiography segmentation: A comprehensive Systematic Literature Review," Eng Appl Artif Intell, vol. 133, p. 108510, 2024, doi: https://doi.org/10.1016/j.engappai.2024.108510.
[12]. A. Karthikeyan, S. Jothilakshmi, and S. Suthir, "Colorectal cancer detection based on convolutional neural networks (CNN) and ranking algorithm," Measurement: Sensors, vol. 31, p. 100976, 2024, doi: https://doi.org/10.1016/j.measen.2023.100976.
[13]. J. Ye, Z. Zhao, E. Ghafourian, A. Tajally, H. A. Alkhazaleh, and S. Lee, "Optimizing the topology of convolutional neural network (CNN) and artificial neural network (ANN) for brain tumor diagnosis (BTD) through MRIs," Heliyon, vol. 10, no. 16, p. e35083, 2024, doi: https://doi.org/10.1016/j.heliyon.2024.e35083.
[14]. A. Shoeibi et al., "Applications of deep learning techniques for automated multiple sclerosis detection using magnetic resonance imaging: A review," Comput Biol Med, vol. 136, p. 104697, 2021, doi: https://doi.org/10.1016/j.compbiomed.2021.104697.
[15]. A. Alijamaat, A. NikravanShalmani, and P. Bayat, "Multiple sclerosis identification in brain MRI images using wavelet convolutional neural networks," Int J Imaging Syst Technol, vol. 31, no. 2, pp. 778–785, Jun. 2021, doi: https://doi.org/10.1002/ima.22492.
[16]. P. Schwab and W. Karlen, "A Deep Learning Approach to Diagnosing Multiple Sclerosis from Smartphone Data," IEEE J Biomed Health Inform, vol. 25, no. 4, pp. 1284–1291, 2021, doi: https://10.1109/JBHI.2020.3021143.
[17]. E. Mohseni and S. M. Moghaddasi, "A Hybrid Approach for MS Diagnosis Through Nonlinear EEG Descriptors and Metaheuristic Optimized Classification Learning," Comput Intell Neurosci, vol. 2022, no. 1, p. 5430528, Jan. 2022, doi: https://doi.org/10.1155/2022/5430528.
[18]. M. P. McGinley, C. H. Goldschmidt, and A. D. Rae-Grant, "Diagnosis and Treatment of Multiple Sclerosis: A Review," JAMA, vol. 325, no. 8, pp. 765–779, Feb. 2021, doi: https://10.1001/jama.2020.26858.
[19]. W. Huang, W. Chen, and X. Zhang, "Multiple sclerosis: Pathology, diagnosis and treatments (Review)," Exp Ther Med, vol. 13, no. 6, pp. 3163–3166, 2017, doi: https://10.3892/etm.2017.4410.
[20]. B. Zakrzewska-Pniewska et al., "Update on diagnosis and treatment of neuromyelitis optica spectrum disorders (NMOSD) — recommendations of Section of Multiple Sclerosis and Neuroimmunology of Polish Neurological Society," Neurol Neurochir Pol, vol. 59, no. 1, pp. 6–19, 2025, doi: https://10.5603/pjnns.100945.
[21]. H. M. Rehan Afzal, S. Li, Y. Feng, M. K. Afzal, and P. Yang, "Enhancing multiple sclerosis diagnosis and prognosis through a dual Patch-Wise CNN architecture," Biomed Signal Process Control, vol. 107, p. 107835, 2025, doi: https://doi.org/10.1016/j.bspc.2025.107835.
[22]. G. Placidi et al., "A Context-Dependent CNN-Based Framework for Multiple Sclerosis Segmentation in MRI," Int J Neural Syst, vol. 35, no. 03, p. 2550006, Dec. 2024, doi: https://10.1142/S0129065725500066.
[23]. S. J. Basha, D. Veeraiah, P. C. Kumar, and P. C. K. Reddy, "Advancing Multiple Sclerosis Diagnosis: A CNN Approach for Personalized Therapy," in 2024 5th International Conference on Electronics and Sustainable Communication Systems (ICESC), 2024, pp. 1926–1931. doi: https://10.1109/ICESC60852.2024.10689766.
[24]. W. Brahmi, I. Jdey, and F. Drira, "Exploring the role of Convolutional Neural Networks (CNN) in dental radiography segmentation: A comprehensive Systematic Literature Review," Eng Appl Artif Intell, vol. 133, p. 108510, 2024, doi: https://doi.org/10.1016/j.engappai.2024.108510.
[25]. A. Karthikeyan, S. Jothilakshmi, and S. Suthir, "Colorectal cancer detection based on convolutional neural networks (CNN) and ranking algorithm," Measurement: Sensors, vol. 31, p. 100976, 2024, doi: https://doi.org/10.1016/j.measen.2023.100976.

[26]. J. Ye, Z. Zhao, E. Ghafourian, A. Tajally, H. A. Alkhazaleh, and S. Lee, "Optimizing the topology of convolutional neural network (CNN) and artificial neural network (ANN) for brain tumor diagnosis (BTD) through MRIs," Heliyon, vol. 10, no. 16, p. e35083, 2024, doi: https://doi.org/10.1016/j.heliyon.2024.e35083.

[27]. A. F. Amiri, S. Kichou, H. Oudira, A. Chouder, and S. Silvestre, "Fault Detection and Diagnosis of a Photovoltaic System Based on Deep Learning Using the Combination of a Convolutional Neural Network (CNN) and Bidirectional Gated Recurrent Unit (Bi-GRU)," 2024. doi: https://10.3390/su16031012.

[28]. M. N. I. Siddique, M. Shafiullah, S. Mekhilef, H. Pota, and M. A. Abido, "Fault classification and location of a PMU-equipped active distribution network using deep convolution neural network (CNN)," Electric Power Systems Research, vol. 229, p. 110178, 2024, doi: https://doi.org/10.1016/j.epsr.2024.110178.

[29]. S. Shinde, A. Himpalnerkar, S. Shendurkar, S. Deshmane, and S. Jadhav, "Cattle Disease Detection using VGG16 CNN Architecture," in 2024 15th International Conference on Computing Communication and Networking Technologies (ICCCNT), 2024, pp. 1–6. doi: https://10.1109/ICCCNT61001.2024.10724717.

[30]. R. Bhuria and S. Gupta, "Transformative Imaging: Enhancing Chest Cancer Detection using VGG16 CNN Architecture," in 2024 3rd International Conference for Advancement in Technology (ICONAT), 2024, pp. 1–6. doi: https://10.1109/ICONAT61936.2024.10775282.

[31]. A. G. V. Sai and R. Puviarasi, "Diabetes detection using VGG16 CNN and ResNet50 CNN algorithm for accuracy, specificity, and sensitivity improvement," AIP Conf Proc, vol. 2816, no. 1, p. 030003, Mar. 2024, doi: https://10.1063/5.0186150.

[32]. L. A. Latumakulita, F. J. Paat, S. Saroyo, I. Karim, I. N. G. A. Astawa, and H. Sirait, "Comparison of MobileNet and VGG16 CNN Architectures for Web-based Starfish Species Identification System," Journal of Applied Data Sciences; Vol 5, No 4: DECEMBER 2024DO - 10.47738/jads.v5i4.456 , Dec. 2024, [Online]. Available: https://bright-journal.org/Journal/index.php/JADS/article/view/456.

[33]. M. T. Hidayat, F. Adiba, M. Yahya, D. D. Andayani, and A. B. Kaswar, "Enhanced Flood Detection on Highways: A Comparative Study of MobileNet and VGG16 CNN Models Based on CCTV Images," in 2024 4th International Conference of Science and Information Technology in Smart Administration (ICSINTESA), 2024, pp. 125–130. doi: https://10.1109/ICSINTESA62455.2024.10747897.

[34]. S. U. Nisa, K. Hamza, and A. Shafiq, "Enhancing Real-Time Detection of Rice Diseases Using an Optimized Deep Learning Model," Plant Protection, vol. 8, no. 4, pp. 679–689, 2024, doi: https://10.33804/pp.008.04.5439.

[35]. S. Shrivastava, S. Rathore, and R. Gedam, "Deep Feature Extraction and Classification of Diabetic Retinopathy Using AlexNet, InceptionV3, and VGG16 CNN Architectures," in Proceedings of the 5th International Conference on the Role of Innovation, Entrepreneurship and Management for Sustainable Development (ICRIEMSD-2024), Atlantis Press, 2024, pp. 80–94. doi: https://10.2991/978-94-6463-612-3_7.

[36]. S. M. Zakariya and M. S. Umar, "Self-Attention Augmented Wasserstein Generative Adversarial Network-based Detection of Brain Alzheimer Disease Using MRI," International Research Journal of Multidisciplinary Scope, vol. 6, no. 1, pp. 1317–1327, Jan. 2025, doi: https://10.47857/irjms.2025.v06i01.02645.

[37]. S. M. Zakariya and M. A. Jamil, "Unsupervised Content based Image Retrieval at Different Precision Level by Combining Multiple Features," J Phys Conf Ser, vol. 1950, no. 1, p. 012059, 2021, doi: https://10.1088/1742-6596/1950/1/012059

